

Secure Wireless Communications in The Multi-user MISO Interference Channel Assisted by Multiple Reconfigurable Intelligent Surfaces

Ya Liu, Jie Yang, Kaizhi Huang, Xiaoli Sun, and Yi Wang

Abstract—This paper exploits reconfigurable intelligent surfaces (RIS) to enhance physical layer security (PLS) in a challenging radio environment. By adjusting the reflecting coefficients, RIS can provide a programmable wireless environment so that the electromagnetic wave can propagate in the desired way. Specifically, we consider a scenario where multiple user pairs communicate simultaneously over the same channel in a multi-user MISO interference channel and each pair of transceivers keeps their confidential information secret from other receivers. We investigate the secrecy rate balance of the system aided by multiple RISs and exploit the additional design degrees of freedom provided by the coordinated RISs to increase the secrecy capacity, achieving secrecy transmission. In particular, we adopt cooperative beamforming among the collaborative transmitters to maximize all users' minimum secrecy rate, achieving the secrecy rate balance. Due to the non-convexity of the formulated optimization problem, we propose alternating optimization (AO) to solve it iteratively and optimize active the transmit beamforming at the transmitters and passive phase shifts at the RISs based on positive semi-definite relaxation (SDR) and successive convex approximation (SCA). In each iteration, we solve a semi-definite programming (SDP) problem and finally get the optimal local solution to the optimization problem. Finally, the simulation results validate that the proposed algorithm is effective and the introduced RISs can significantly enhance the system secrecy performance compared to conventional baseline schemes.

Index Terms—Physical layer security, reconfigurable intelligent surface, secrecy rate, semi-definite relaxation, successive convex approximation.

I. INTRODUCTION

AS a powerful supplement to the conventional high-level cryptographic encryption methods, physical layer security (PLS) uses the physical characteristics of the wireless channels (fading, noise, interference) to restrict the eavesdroppers from approaching confidential information, which provides a lightweight and effective secrecy solution [1]–[3]. In the research of PLS, the authors usually used cooperative relay [4], artificial noise-aided beamforming [5], and

cooperative jamming [6] to improve the security of wireless communication systems. However, relays or other auxiliary equipment deployment brings additional cost consumption. Moreover, Cooperative interference and artificial noise consume extra power. The uncontrollable wireless environment limits electromagnetic wave transmission. If the wireless channel can be actively regulated, it will bring great potential to the development of secure communication.

Recently, reconfigurable intelligent surfaces (RIS) is expected to provide a cost-effective means for secure transmission [7]–[9]. RIS can effectively be programmed to manipulate the waveform (phase, amplitude, frequency, polarization, etc.) of incident electromagnetic waves in a customizable manner without complex coding and radio frequency (RF) processing [10]–[12]. A RIS is typically constructed by the printed circuit board (PCB), consisting of a reflective unit layer, a copper plate, and a control circuit board. Each reflecting element of the RIS is implemented by reflective arrays that use varactor diodes with the resonant frequency electronically controlled and is composed of full metal sheets on the bottom layers and metal patches on the top layers of the PCB dielectric substrates [13]. By elaborately adjusting the phase shifts of the reflecting elements, the desired signals can be constructively enhanced, and unfavorable signals are destructively mitigated, such as multi-user interference or signal leakage to eavesdroppers.

RIS enhanced PLS transmission has attracted extensive attention in recent years. The authors in [14], [15] considered secure communication with a single eavesdropping node in the MISO system. By jointly designing the transmit beamforming of the access point (AP) and the passive reflection beamforming of the RIS, the confidentiality rate of the legal communication link can be maximized. The simultaneous transmission and reflection RIS was exploited to improve the security of the MISO system in [16]. And the authors maximized the weighted sum secrecy rate by jointly designing the beamforming and the transmitting and reflecting coefficients. The authors in [17] studied the secure communication of the RIS-assisted MISO system and introduced artificial noise (AN) in the presence of eavesdroppers. The RIS phase shift matrix, BS transmission beamforming, and the covariance matrix of the AN were jointly optimized to maximize the sum reachable secrecy rate. The authors in [18] considered a practical scenario where multiple RISs are deployed to serve multiple legitimate users. The transmit beamforming of AP, AN covariance matrix, and RIS phase shift matrix

Manuscript received April 17, 2022 revised June 7, 2022; approved for publication by Zhengyu Zhu, Guest Editor, July 6, 2022.

This research was funded by the National Natural Science Foundation of China, grant number 61871404 and Training Program for Young Scholar of Henan Province for Colleges and Universities under Grand 2020GGJS172 (Corresponding author: Jie Yang)

Ya Liu, Jie Yang, Kaizhi Huang, and Xiaoli Sun are with Information Engineering University, Zhengzhou, 450002, China. Ya Liu and Yi Wang are also with Zhengzhou University of Aeronautics, Zhengzhou 450015, China. email: liuya2014@zua.edu.cn, yj_csu@126.com, huangkaizhi@tsinghua.org.cn, lgdxsunxiaoli@sina.com, yiwang@zua.edu.cn

J. Yang is the corresponding author.

Digital Object Identifier: 10.23919/JCN.2022.000027

Creative Commons Attribution-NonCommercial (CC BY-NC).

This is an Open Access article distributed under the terms of Creative Commons Attribution Non-Commercial License (<http://creativecommons.org/licenses/by-nc/3.0>) which permits unrestricted non-commercial use, distribution, and reproduction in any medium, provided that the original work is properly cited.

were jointly optimized to maximize the sum secrecy rate based on alternating optimization (AO), successive convex approximation (SCA), and semi-positive definite relaxation (SDR) methods. The author in [19] studied the RIS-assisted PLS transmission in the scenario of random deployment of multiple legitimate users and a multi-antenna eavesdropper by using the random geometry theory.

However, the existing researches consider the RIS-assisted network model with a single BS, and the security requirements are relatively simple. In the future mobile communication network, with the improvement of data transmission rate and node density and the miniaturization of cell size, the resulting interference usually has a more severe impact. Therefore, it is urgent to suppress interference or minimize information leakage to those unintended recipients [20], especially in dense networks or for cell-edge users. This paper investigates the multi-user MISO system allowing multiple user pairs to communicate simultaneously over the same channel. Each BS expects to transmit its independent information to the corresponding target receiver safely and reliably. That is, each BS sends information to only one corresponding target user. Mutual interference among the receivers exists in the system, and other receivers are regarded as potential eavesdroppers. To improve the security of information transmission in this system, we use multiple cooperative RISs to enhance PLS by providing additional degrees of freedom (DoF). So far, very few works consider the RIS-assisted interference channel scenarios [21]–[24]. The authors in [21] considered a RIS-aided MISO interference channel, where each of the transmitter-receiver pairs is aided by one RIS, and proposed a joint transmit and reflective beamforming design scheme to characterize the achievable rate region based on a second-order cone program (SOCP) and SDR methods. The authors in [22] consider a RIS-assisted MISO interference channel scenario and design the digital beamforming vectors at transmitters and the analog phase shift matrix at the RIS based on a deep reinforcement learning (DRL)-empowered algorithm for maximizing the achievable sum rate. The authors in [23] study a RIS-assisted two-user MISO system, where a multi-antenna base station (BS) serves a single-antenna user with the help of a RIS in the presence of interference from another transceiver pair. However, the interference channel was assisted by one RIS, and the achievable sum rate of the system was considered in [22] and [23]. The authors in [24] studied a co-channel communication system composed of multiple paired transceivers assisted by a single RIS. They proposed a RIS passive reflection coefficient allocation method based on Riemannian manifold optimization to minimize the total interference of all paired users in the system. However, the secrecy of information transmission between paired users has not been analyzed.

Based on the above analysis, the main contributions of this paper are as follows:

1) This paper studies the PLS transmission in the multi-user MISO interference channel with confidential information assisted by multi RISs. To enhance the secrecy of data streams, we deploy multiple RISs to adjust the beams which transmit signals in specific directions, realizing the flexible focusing

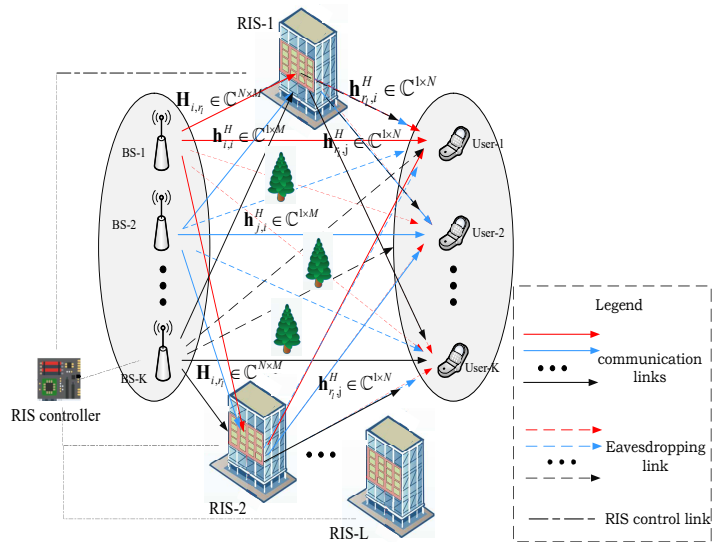


Fig. 1. Multi-user MISO interference channel model with confidential information aided by RISs.

of beams in different directions. Multiple RISs expand the coverage of signals and increase the secrecy capacity, which realizes secure transmission.

2) We assume the ideal CSI is known [25], [26]. To ensure the fairness of each user's secure communication in the system, we study the balance of secrecy rate. An iterative optimization-based collaborative beamforming (CB) method is proposed to maximize the minimum secrecy rate by jointly optimizing each BS's beamforming vector and RIS reflection coefficient matrix.

3) An efficient alternating optimization (AO)-based method is proposed to solve non-convexity since the transmit beamforming vector and the RIS reflection coefficient matrix are coupled. Then, we design the transmit beamforming and RIS phase-shifting based on SCA and SDR. The optimal local solution to the optimization problem is finally obtained after solving a semi-definite program (SDP) problem in each iteration. The convergence of the iterative optimization algorithm is proved and verified by simulations.

The rest of the paper is organized as follows. Section II describes the system model and problems discussed in this paper. In Section III, we optimize the design of transmission scheme. Section IV designs the transmission strategy under discrete phase shifts, and Section V presents the simulation results. Section VI draws the conclusions.

II. SYSTEM MODEL AND PROBLEM FORMULATION

A. System Model

As shown in Fig. 1, we consider a multi-user MISO interference channel with K pairs of transceivers. Each BS is equipped with M antennas, and each receiver is a single-antenna device. Each BS sends independent information to the corresponding receiver by beamforming, and the information is confidential to other non-target users. Therefore, the

remaining $k - 1$ users are potential internal eavesdroppers for any paired transceivers.

The traditional scheme optimizes the beamforming vector at the transmitter and aims the beam at the corresponding user to reduce the risk of information leakage. However, security leakage increases with the number of users due to the limited number of antennas at the BS. In this paper, L RISs are deployed around BSs, which are remotely controlled by the BS's private wired/wireless channel. Each RIS consists of N reflective elements, enhancing the desired signal and suppressing eavesdropping signals from other users by phase-shift processing. Moreover, each reflective element can adjust the phase independently.

After introducing RISs, the communication links from the BS i to the user i are composed of a direct link and reflective links, where the direct link is defined as $\mathbf{h}_{i,i}^H \in \mathbb{C}^{1 \times M}$, the reflective link from the sender i to the RIS l is $\mathbf{H}_{i,r_l} \in \mathbb{C}^{N \times M}$, and the IRS l to the user i is $\mathbf{h}_{r_l,i}^H \in \mathbb{C}^{1 \times N}$. Similarly, the eavesdropping links for the user j who eavesdrops on the private information of the paired transceiver i also consist of a direct link and reflective links. The direct link $\mathbf{h}_{j,i}^H \in \mathbb{C}^{1 \times M}$, the reflective link from the BS i to the RIS l $\mathbf{H}_{i,r_l} \in \mathbb{C}^{N \times M}$, and the channel from IRS l to user j $\mathbf{h}_{r_l,j}^H \in \mathbb{C}^{1 \times N}$ are defined. The reflection coefficient matrix of RIS is defined as $\Phi_l = \text{diag}(\beta_1 e^{j\theta_1}, \beta_2 e^{j\theta_2}, \dots, \beta_N e^{j\theta_N})$, where $\text{diag}(\cdot)$ denotes a diagonal matrix. We assume the reflection amplitude $\beta_n = 1$ and the phase shift $\theta_n \in [0, 2\pi]$. Generally, due to the hardware limitation, the phase adopts a multi-bit discrete quantization. Assuming the number of quantization bits is B , the phase shift can be expressed as $\xi = \{n2\pi/2^B, n = 0, 1, 2, \dots, 2^B - 1\}$.

For the BS j , the transmitted signal can be expressed as:

$$\mathbf{x}_j = \mathbf{w}_j s_j, \quad (1)$$

where $s_j \sim \mathcal{CN}(0, 1)$ is the transmitted signal, $\mathbf{w}_j \in \mathbb{C}^N$ is the beamforming vector for the j th paired BS and user, and $j \in \kappa \triangleq \{1, \dots, K\}$.

The received signal of the corresponding j th user can be expressed as:

$$\begin{aligned} y_j = & (\mathbf{h}_{j,j}^H + \sum_{l=1}^L \mathbf{h}_{r_l,j}^H \Phi_l \mathbf{H}_{j,r_l}) \mathbf{w}_j s_j \\ & + \sum_{i=1, i \neq j}^K (\mathbf{h}_{j,i}^H + \sum_{l=1}^L \mathbf{h}_{r_l,j}^H \Phi_l \mathbf{H}_{i,r_l}) \mathbf{w}_i s_i + n_j, j \in \kappa, \end{aligned} \quad (2)$$

where $n_j \sim \mathcal{CN}(0, \sigma_j^2)$ denotes the additive white Gaussian noise (AWGN) of the j th user.

Define $\mathbf{V}_l^H = [v_{l1}, v_{l2}, \dots, v_{lN}]$, where $v_{ln} = e^{j\theta_n}$, then we can obtain

$$\mathbf{h}_{r_l,j}^H \Phi_l \mathbf{H}_{j,r_l} = \mathbf{V}_l^H \mathbf{H}_{j,r_l}, \quad (3)$$

$$\mathbf{h}_{r_l,i}^H \Phi_l \mathbf{H}_{i,r_l} = \mathbf{V}_l^H \mathbf{H}_{i,r_l}. \quad (4)$$

The cascaded channels can be represented as $\mathbf{H}_{j,r_l,j} = \text{diag}(\mathbf{h}_{r_l,j}^H) \mathbf{H}_{j,r_l}$ and $\mathbf{H}_{i,r_l,j} = \text{diag}(\mathbf{h}_{r_l,j}^H) \mathbf{H}_{i,r_l}$, respectively. Then the sum in (2) can be further expressed as

$$\sum_{l=1}^L \mathbf{h}_{r_l,j}^H \Phi_l \mathbf{H}_{j,r_l} = \sum_{l=1}^L \mathbf{V}_l^H \mathbf{H}_{j,r_l} = \mathbf{V}^H \mathbf{H}_{j,r_j}, \quad (5)$$

$$\sum_{l=1}^L \mathbf{h}_{r_l,i}^H \Phi_l \mathbf{H}_{i,r_l} = \sum_{l=1}^L \mathbf{V}_l^H \mathbf{H}_{i,r_l} = \mathbf{V}^H \mathbf{H}_{i,r_j}, \quad (6)$$

where

$\mathbf{V}^H = [\mathbf{V}_1^H, \mathbf{V}_2^H, \dots, \mathbf{V}_L^H]$, and $\mathbf{H}_{j,r_j} = [\mathbf{H}_{j,r_1,j}, \mathbf{H}_{j,r_2,j}, \dots, \mathbf{H}_{j,r_L,j}]^T$, and $\mathbf{H}_{i,r_j} = [\mathbf{H}_{i,r_1,j}, \mathbf{H}_{i,r_2,j}, \dots, \mathbf{H}_{i,r_L,j}]^T$. The signal received by user j can be re-expressed as

$$\begin{aligned} y_j = & (\mathbf{h}_{j,j}^H + \mathbf{V}^H \mathbf{H}_{j,r_j}) \mathbf{w}_j s_j \\ & + \sum_{i=1, i \neq j}^K (\mathbf{h}_{j,i}^H + \mathbf{V}^H \mathbf{H}_{i,r_j}) \mathbf{w}_i s_i + n_j, j \in \kappa. \end{aligned} \quad (7)$$

We further express $\tilde{\mathbf{H}}_{j,j}$, $\tilde{\mathbf{H}}_{j,i}$, and $\tilde{\mathbf{V}}^H$ as $\tilde{\mathbf{H}}_{j,j} = \begin{bmatrix} \mathbf{H}_{j,r_j} \\ \mathbf{h}_{j,j}^H \end{bmatrix}$, $\tilde{\mathbf{H}}_{j,i} = \begin{bmatrix} \mathbf{H}_{i,r_j} \\ \mathbf{h}_{j,i}^H \end{bmatrix}$, and $\tilde{\mathbf{V}}^H = e^{j\bar{w}} [\mathbf{V}^H, 1]$, respectively. So we can get $\tilde{\mathbf{H}}_{j,j}^H = \tilde{\mathbf{V}}^H \tilde{\mathbf{H}}_{j,j}$ and $\tilde{\mathbf{H}}_{j,i}^H = \tilde{\mathbf{V}}^H \tilde{\mathbf{H}}_{j,i}$, where $\bar{w} \in [0, 2\pi]$ is the introduced auxiliary constant. We can see that \bar{w} does not affect the optimal solution from the subsequent derivation, and the solution constraints of $\tilde{\mathbf{V}}^H$ are relaxed. We can deduce \mathbf{V}^H after solving $\tilde{\mathbf{V}}^H$.

Finally, the received signal can be expressed as

$$y_j = \tilde{\mathbf{H}}_{j,j}^H \mathbf{w}_j s_j + \sum_{i=1, i \neq j}^K \tilde{\mathbf{H}}_{j,i}^H \mathbf{w}_i s_i + n_j. \quad (8)$$

B. Problem Formulation

Through the above matrix transformation, we can see that $\tilde{\mathbf{H}}_{j,i}^H$ is the equivalent channel vector from the BS i to the user j , and $\tilde{\mathbf{H}}_{j,j}^H$ is the equivalent channel vector from the BS j to the user j . The signal model in (8) can be regarded as a virtual multiple access channel. The lemma for the achievable rate of the MAC channel is given as follows [27].

Lemma 1: For a multiple access channel with K users, a continuous interference cancellation strategy is used for decoding, which can reach any boundary point in the capacity domain. Given the decoding order $(\pi(1), \pi(2), \dots, \pi(K))$, that is, $\pi(1)$ is decoded first, then $\pi(2)$ is decoded, and so on, then the reachable rate of user $\pi(j)$ is

$$R_{\pi(j)} = \log_2 \left(1 + \frac{\mathbf{h}_{\pi(j)}^H \mathbf{Q}_{\pi(j)} \mathbf{h}_{\pi(j)}}{1 + \sum_{i=j+1}^K \mathbf{h}_{\pi(i)}^H \mathbf{Q}_{\pi(i)} \mathbf{h}_{\pi(i)}} \right), \quad (9)$$

where $\mathbf{h}_{\pi(j)}$ and $\mathbf{Q}_{\pi(j)}$ represent the corresponding channel vector and the covariance matrix of the signal, respectively.

According to Lemma 1, the decoding order determines the achievable information rate. Here, we assume that user j first

decodes its target information s_j and other signals are regarded as interference. The channel capacity of user j is

$$C_j = \log_2 \left(1 + \frac{|\hat{\mathbf{H}}_{j,j}^H \mathbf{w}_j|^2}{1 + \sum_{i \neq j} |\hat{\mathbf{H}}_{j,i}^H \mathbf{w}_i|^2} \right), j \in \kappa. \quad (10)$$

On the other hand, considering the worst case, user i will decode s_j ($i \neq j$) at the end in order to get as much information about it as possible. In this case, the channel capacity of the eavesdropped information s_j is

$$C_{eij} = \log_2 \left(1 + \left| \hat{\mathbf{H}}_{i,j}^H \mathbf{w}_j \right|^2 \right), \forall i \neq j, j \in \kappa. \quad (11)$$

According to the definition of secrecy rate (10) and (11), the achievable secrecy rate of user j is

$$C_{sj} = C_j - \max_{i \neq j} C_{eij}, \forall j \in \kappa. \quad (12)$$

In order to ensure that all the users receive secrecy services fairly, we maximize the all users' minimum secrecy rate with the limited transmit power at BSs. The problem of secrecy rate balance can be formulated as follows

$$\begin{aligned} & \max_{\{\mathbf{w}_j\}, \{\mathbf{V}_l^H\}} \min C_{sj} \\ & \text{s.t. } \|\mathbf{w}_j\|^2 \leq P_j, \forall j \in \kappa \\ & |v_{ln}| = 1, n = 1, 2, \dots, N+1, l = 1, 2, \dots, L, \end{aligned} \quad (13)$$

where P_j is the maximum transmission power of the BS j .

III. OPTIMIZATION DESIGN OF THE TRANSMISSION STRATEGY

Assuming that the BSs know the ideal CSI and multiple BSs cooperate, a coordinated beamforming method is used to maximize the minimum user secrecy rate. Substitute (10)–(12) into (13), and we can express the balance problem of secrecy rate as

$$\begin{aligned} & \max_{\{\mathbf{w}_j\}, \{\mathbf{V}_l^H\}} \min_{j \in \kappa} (f(\mathbf{w}_j, \mathbf{V}_l^H)) \\ & \text{s.t. } \|\mathbf{w}_j\|^2 \leq P_j, \forall j \in \kappa \\ & |v_{ln}| = 1, n = 1, 2, \dots, N+1, l = 1, 2, \dots, L, \end{aligned} \quad (14)$$

where $f(\mathbf{w}_j, \mathbf{V}_l^H)$ is shown at the bottom of this page. It is difficult to solve the above problem. First, the variables \mathbf{w}_j and \mathbf{V}_l^H are coupled. Second, the problem is non-convex due to logarithm and fraction operations. We use AO to solve the coupled optimization variables, and then iterate until the objective function converges. At the same time, loose variables are introduced to transform non-convex problems into convex ones.

$$f(\mathbf{w}_j, \mathbf{V}_l^H) = \log_2 \left(1 + \frac{|\tilde{\mathbf{V}}^H \tilde{\mathbf{H}}_{j,j} \mathbf{w}_j|^2}{1 + \sum_{l \neq j} |\tilde{\mathbf{V}}^H \tilde{\mathbf{H}}_{j,l} \mathbf{w}_l|^2} \right) - \max_{i \neq j} \log_2 (1 + |\tilde{\mathbf{V}}^H \tilde{\mathbf{H}}_{i,j} \mathbf{w}_j|^2) \quad (15)$$

A. Optimize \mathbf{w}_j given \mathbf{V}_l^H

First, optimize the beamforming vector \mathbf{w}_j with the fixed phase shift matrix \mathbf{V}_l^H of each RIS. Define $\hat{\mathbf{H}}_{j,i}^H = \hat{\mathbf{H}}_{j,i} \hat{\mathbf{H}}_{j,i}^H$ and $\mathbf{W}_i = \mathbf{w}_i \mathbf{w}_i^H, \forall i, j \in \kappa$, then $\hat{\mathbf{H}}_{j,i}^H \succeq 0, \mathbf{W}_i \succeq 0$, $\text{Rank}(\hat{\mathbf{H}}_{j,i}^H) = 1$, and $\text{Rank}(\mathbf{W}_i) = 1$. According to the properties of the trace of the matrix, we get

$$|\tilde{\mathbf{V}}^H \mathbf{H}_{j,i} \mathbf{w}_i|^2 = \text{Tr}(\hat{\mathbf{H}}_{j,i}^H \mathbf{W}_i), \forall i, j \in \kappa, \quad (16)$$

where $\text{Tr}(\cdot)$ represents the trace of a matrix. Substitute (16) into (14), we get

$$\begin{aligned} & \max_{\{\mathbf{W}_j\}} \min_{j \in \kappa} \left\{ \log_2 \left(1 + \frac{\text{Tr}(\hat{\mathbf{H}}_{j,j}^H \mathbf{W}_j)}{1 + \sum_{l \neq j} \text{Tr}(\hat{\mathbf{H}}_{j,l}^H \mathbf{W}_l)} \right) \right. \\ & \quad \left. - \max_{i \neq j} \log_2 (1 + \text{Tr}(\hat{\mathbf{H}}_{i,j}^H \mathbf{W}_j)) \right\} \end{aligned} \quad (17a)$$

$$\text{s.t. } \text{Tr}(\mathbf{W}_j) \leq P_j, \forall j \in \kappa \quad (17b)$$

$$\mathbf{W}_j \succeq 0, \forall j \in \kappa \quad (17c)$$

$$\text{Rank}(\mathbf{W}_j) = 1, \forall j \in \kappa. \quad (17d)$$

We introduce slack variables φ_j and $u_{i,j}$ in order to simplify (17) and the above optimization problem is equivalent to

$$\max_{\{\mathbf{W}_j\}} \min_{j \in \kappa} \varphi_j - u_{i,j} \quad (18a)$$

$$\text{s.t. } \varphi_j \leq \log_2 \left(1 + \frac{\text{Tr}(\hat{\mathbf{H}}_{j,j}^H \mathbf{W}_j)}{1 + \sum_{l \neq j} \text{Tr}(\hat{\mathbf{H}}_{j,l}^H \mathbf{W}_l)} \right), \forall j \in \kappa \quad (18b)$$

$$\log_2 (1 + \text{Tr}(\hat{\mathbf{H}}_{i,j}^H \mathbf{W}_j)) \leq u_{i,j}, \forall j \neq i, j, i \in \kappa \quad (18c)$$

$$(17b), (17c), (17d). \quad (18d)$$

It can be proved that the equations in (18b) and (18c) are valid at the optimal solutions. Otherwise, the equations can always be established by increasing φ_j and decreasing $u_{i,j}$ without at least reducing the optimal solutions. Therefore, (17) and (18) are equivalent. Further, we will employ SDR and SCA to obtain the optimal solutions.

1) Positive Semi-definite Relaxation

After introducing auxiliary variables z, t_j , and $v_{i,j}$ and dropping the rank-one constraint, (18) can be equivalently

expressed as

$$\max_{\{\mathbf{W}_j\}} z \quad (19a)$$

$$\text{s.t. } z \leq \varphi_j - u_{i,j}, \forall j \neq i, j, i \in \kappa \quad (19b)$$

$$t_j \leq \frac{\text{Tr}(\hat{\mathbf{H}}_{j,j}^H \mathbf{W}_j)}{1 + \sum_{l \neq j} \text{Tr}(\hat{\mathbf{H}}_{j,l}^H \mathbf{W}_l)}, \forall j \in \kappa \quad (19c)$$

$$\varphi_j \leq \log_2(1 + t_j), \forall j \in \kappa \quad (19d)$$

$$1 + \text{Tr}(\hat{\mathbf{H}}_{i,j}^H \mathbf{W}_j) \leq v_{i,j}, \forall j \neq i, j, i \in \kappa \quad (19e)$$

$$\log_2(v_{i,j}) \leq u_{i,j}, \forall j \neq i, j, i \in \kappa \quad (19f)$$

$$(17b), (17c), (17d). \quad (19g)$$

Similar to the above description, we can prove that (18) and (19) are also equivalent. It can be seen that the objective function of (19) is linear, but constraints (19c), (19f), and (16c) are non-convex, which makes it difficult to solve. For the rank-one constraint in (17d), we directly discard the non-convex constraint based on SDR and relax the solution sets of (19). Therefore, we focus on the non-convex constraints in (19c), (19f).

2) Iterative Optimization based on SCA

We deal with the non-convex constraints in (19c) and (19f) based on SCA. Introducing slack variables $x_{j,1}$ and $x_{j,2}$, (19c) can be equivalently transformed into

$$x_{j,1} \leq \text{Tr}(\hat{\mathbf{H}}_{j,j}^H \mathbf{W}_j), \forall j \in \kappa, \quad (20a)$$

$$1 + \sum_{l \neq j} \text{Tr}(\hat{\mathbf{H}}_{j,l}^H \mathbf{W}_l) \leq x_{j,2}, \forall j \in \kappa, \quad (20b)$$

$$t_j \leq \frac{x_{j,1}}{x_{j,2}}, \forall j \in \kappa. \quad (20c)$$

Obviously, the constraints in (20a) and (20b) are convex. In addition, according to (19e), it can be seen that (20b) is equivalent to

$$1 + \sum_{l \neq j} (v_{j,l} - 1) \leq x_{j,2}, \forall j \in \kappa. \quad (21)$$

Now, we solve the non-convexity in (20c) based on SCA. Firstly, the non-convex constraints are replaced with conservative convex constraints in the SCA technology. Then, we solve convex optimization problems similar to the original problem in an iterative manner. The obtained solution can be approximately regarded as the solution of the original non-convex problem when the final convergence condition is established. Suppose that $f(x) \leq 0$ is a non-convex constraint in an optimization problem, where $f(x)$ is a non-convex function. Next, we analyze how to replace the non-convex constraint $f(x) \leq 0$ with an approximate convex constraint. Find a convex function $F(x, \lambda)$, λ is a given parameter that satisfies $f(x) \leq F(x, \lambda)$, that is, $F(x, \lambda)$ is a convex upper bound function of $f(x)$. $\lambda = \phi(x)$ should satisfy the following equations

$$f(x) = F(x, \phi(x)), \quad \nabla f(x) = \nabla F(x, \phi(x)), \quad (22)$$

where $\nabla f(x)$ is the gradient of $f(x)$. Then, in the n th iteration, $f(x)$ is replaced by the convex function $F(x, \lambda^{(n)})$. we use a convex constraint $F(x, \lambda^{(n)}) \leq 0$ to replace $f(x) \leq 0$, where $\lambda^{(n)}$ is updated according to the optimal solution $x^{(n-1)}$

of x in the $(n-1)$ th iteration, i.e., $\lambda^{(n)} = \phi(x^{(n-1)})$. The constraint (20c) is equivalent to

$$f_1(t_j, x_{j,2}) \triangleq t_j x_{j,2} \leq x_{j,1}, \forall j \in \kappa. \quad (23)$$

Obviously, $f_1(t_j, x_{j,2})$ is non-convex. Based on SCA, we first find a convex upper bound function of $f_1(t_j, x_{j,2})$. Define the following convex function with respect to t_j and $x_{j,2}$,

$$F_1(t_j, x_{j,2}, \eta_j) \triangleq \frac{1}{2}(\eta_j t_j^2 + \frac{x_{j,2}^2}{\eta_j}), \quad (24)$$

where $\eta_j > 0$ is a constant. We can verify that

$$F_1(t_j, x_{j,2}, \eta_j) - f_1(t_j, x_{j,2}) \triangleq \frac{1}{2}(\sqrt{\eta_j} t_j - \frac{x_{j,2}}{\sqrt{\eta_j}})^2 \geq 0. \quad (25)$$

The convex function $F_1(t_j, x_{j,2}, \eta_j)$ is the upper bound of the non-convex function $f_1(t_j, x_{j,2})$. In addition, it can be further verified that the constraint conditions of (22) are satisfied when $\eta_j > x_{j,2}/t_j$. Therefore, (20c) can be replaced by the following convex constraint in the n th iteration.

$$\frac{1}{2}(\eta_j^{(n)} t_j^2 + \frac{x_{j,2}^2}{\eta_j^{(n)}}) \leq x_{j,1}, \forall j \in \kappa \quad (26)$$

where $\eta_j^{(n)} = x_{j,2}^{(n-1)}/t_j^{(n-1)}$, $x_{j,2}^{(n-1)}$, and $t_j^{(n-1)}$ are the optimal solutions of $x_{j,2}$ and t_j in the $(n-1)$ th iteration, respectively.

In (19f), we can see the function $f_2(v_{i,j}) \triangleq \log_2(v_{i,j})$ is concave for $v_{i,j}$. Its first-order Taylor expansion at point $\varepsilon_j > 0$ is expressed as

$$F_2(v_{i,j}, \varepsilon_{i,j}) \triangleq \log_2(v_{i,j}) + \frac{v_{i,j} - \varepsilon_{i,j}}{\varepsilon_{i,j} \ln 2}. \quad (27)$$

According to the properties of the concave function, we know that $F_2(v_{i,j}, \varepsilon_{i,j}) - f_2(v_{i,j}) \geq 0$, i.e., $F_2(v_{i,j}, \varepsilon_{i,j})$ is the upper bound of $f_2(v_{i,j})$. In addition, the constraints of (22) are satisfied when $\varepsilon_j = v_{i,j}$. Therefore, the (19f) can be replaced by the following convex constraint in the n th iteration,

$$\log_2(\varepsilon_{i,j}^{(n)}) + \frac{v_{i,j} - \varepsilon_{i,j}^{(n)}}{\varepsilon_{i,j}^{(n)} \ln 2} \leq u_{i,j}, \forall j \neq i, j, i \in \kappa, \quad (28)$$

where $\varepsilon_{i,j}^{(n)} = v_{i,j}^{(n-1)}$, $v_{i,j}^{(n-1)}$ is the optimal solution of $v_{i,j}$ in the $(n-1)$ th iteration. Therefore, the non-convex constraint in (19f) is transformed into an equivalent convex constraint. Next, we find a locally optimal solution to the non-convex problem by iterative optimization. We solve the following SDP problem in the n th iteration,

$$R_s^{(n)} = \max_{\{\mathbf{W}_j > 0\}} z \quad (29a)$$

$$\text{s.t. } x_{j,1} \leq \text{Tr}(\hat{\mathbf{H}}_{j,j}^H \mathbf{W}_j), \forall j \in \kappa \quad (29b)$$

$$1 + \sum_{l \neq j} (v_{j,l} - 1) \leq x_{j,2}, \forall j \in \kappa \quad (29c)$$

$$\frac{1}{2}(\eta_j^{(n)} t_j^2 + \frac{x_{j,2}^2}{\eta_j^{(n)}}) \leq x_{j,1}, \forall j \in \kappa \quad (29d)$$

$$\varphi_j \leq \log_2(1 + t_j), \forall j \in \kappa \quad (29e)$$

$$\log_2(\varepsilon_{i,j}^{(n)}) + \frac{v_{j,i} - \varepsilon_{i,j}^{(n)}}{\varepsilon_{i,j}^{(n)} \ln 2} \leq u_{i,j}, \forall j \neq i, j, i \in \kappa \quad (29f)$$

$$(19b), (19e), (17b), (17c), \quad (29g)$$

Algorithm 1 The proposed algorithm based on SCA for solving (29)

- 1: **Input:** the maximum number of iterations N' , the initial value $(x_{j,2}^{(0)}, t_j^{(0)}, v_{i,j}^{(0)})$
- 2: **Output:** The optimal solution $\{\mathbf{W}_j^*\}$
- 3: Initialize $n = 0$
- 4: **repeat**
- 5: The optimal solution to (29) based on the CVX tool is $(x_{j,2}^*, t_j^*, v_{i,j}^*)$;
- 6: Update $n = n + 1$.
- 7: Let $(x_{j,2}^{(n)}, t_j^{(n)}, v_{i,j}^{(n)}) = (x_{j,2}^*, t_j^*, v_{i,j}^*)$;
- 8: **until** The fractional decrease of the objective value is below the error ε or the iteration number meets $n = N'$

where $\eta_j^{(n)} = x_{j,2}^{(n-1)} / t_j^{(n-1)}$, $\varepsilon_{i,j}^{(n)} = v_{i,j}^{(n-1)}$. We can solve the above SDP problem using an optimization package based on interior point methods, such as CVX.

3) Gaussian Randomization

In Algorithm 1, we drop the rank-one constraint. The optimal solution $\{\mathbf{W}_j^*\}$ may not satisfy $\text{Rank}(\mathbf{W}_j^*) = 1, \forall j \in \mathcal{K}$. If the rank of \mathbf{W}_j^* is 1, the corresponding beamforming vector can be obtained by matrix decomposition, i.e., $\mathbf{W}_j^* = \bar{\mathbf{w}}_j \bar{\mathbf{w}}_j^H, \forall j \in \mathcal{K}$. If at least one \mathbf{W}_j^* whose rank is not 1, the beamforming vector can be extracted by the Gaussian randomization [28].

B. Optimize \mathbf{V}_l^H given \mathbf{w}_j

Next, we optimize \mathbf{V}_l^H under the given \mathbf{w}_j based on the AO scheme. For a given \mathbf{w}_j , define $\tilde{\mathbf{H}}_{j,i} = \tilde{\mathbf{H}}_{j,i} \mathbf{w}_i$, $\hat{\mathbf{H}}_{j,i} = \tilde{\mathbf{H}}_{j,i} \tilde{\mathbf{H}}_{j,i}^H, \forall j, i \in \mathcal{K}$, and $\hat{\mathbf{V}} = \tilde{\mathbf{V}} \tilde{\mathbf{V}}^H$. We see that $\hat{\mathbf{H}}_{j,i} \succeq 0$, $\hat{\mathbf{V}} \succeq 0$, and $\text{Rank}(\hat{\mathbf{V}}) = 1$. The diagonal element of the matrix $\hat{\mathbf{V}}$ is always 1. We can deduce that

$$\left| \tilde{\mathbf{V}}^H \tilde{\mathbf{H}}_{j,i} \tilde{\mathbf{w}}_i \right|^2 = \text{Tr}(\hat{\mathbf{H}}_{j,i} \hat{\mathbf{V}}), \forall j, i \in \mathcal{K}. \quad (30)$$

Then the above optimization problem is equivalent to

$$\max_{\hat{\mathbf{V}}} \min_{\substack{\forall j \in \mathcal{K} \\ i \neq j}} \left\{ \log_2 \left(1 + \frac{\text{Tr}(\hat{\mathbf{H}}_{j,j} \hat{\mathbf{V}})}{1 + \sum_{l \neq j} \text{Tr}(\hat{\mathbf{H}}_{j,l} \hat{\mathbf{V}})} \right) - \max_{i \neq j} \log_2(1 + \text{Tr}(\hat{\mathbf{H}}_{i,j} \hat{\mathbf{V}})) \right\} \quad (31a)$$

$$\text{s.t. } \hat{\mathbf{V}} \succ 0 \quad (31b)$$

$$\text{Rank}(\hat{\mathbf{V}}) = 1 \quad (31c)$$

$$\hat{\mathbf{V}}_{n,n} = 1, n = 1, 2, \dots, L(N+1). \quad (31d)$$

1) Solve the Optimal Matrix $\hat{\mathbf{V}}$

We introduce slack variables ψ_j and $m_{i,j}$ to simplify (31), then (31) is equivalent to

$$\max_{\hat{\mathbf{V}}} \min_{\forall j \in \mathcal{K}} \psi_j - m_{i,j} \quad (32a)$$

$$\text{s.t. } \psi_j \leq \log_2 \left(1 + \frac{\text{Tr}(\hat{\mathbf{H}}_{j,j} \hat{\mathbf{V}})}{1 + \sum_{l \neq j} \text{Tr}(\hat{\mathbf{H}}_{j,l} \hat{\mathbf{V}})} \right), \forall j \in \mathcal{K} \quad (32b)$$

$$\log_2(1 + \text{Tr}(\hat{\mathbf{H}}_{i,j} \hat{\mathbf{V}})) \leq m_{i,j}, \forall j \neq i, j, i \in \mathcal{K} \quad (32c)$$

$$(31b), (31c), (31d). \quad (32d)$$

Algorithm 2 Optimization scheme for solving (34)

- 1: **Input:** the maximum number of iterations N' , the initial value $(x'_{j,2}{}^{(0)}, d_j^{(0)}, \tau_{i,j}^{(0)})$
- 2: **Output:** The optimal solution $\{\hat{\mathbf{V}}^*\}$
- 3: Initialize $n = 0$
- 4: **repeat**
- 5: The optimal solution to (34) based on the CVX tool is $(x'_{j,2}{}^*, d_j^*, \tau_{i,j}^*)$;
- 6: Update $n = n + 1$.
- 7: Let $(x'_{j,2}{}^{(n)}, d_j^{(n)}, \tau_{i,j}^{(n)}) = (x'_{j,2}{}^*, d_j^*, \tau_{i,j}^*)$;
- 8: **until** The fractional decrease of the objective value is below the error ε or the iteration number meets $n = N'$;

Similar to the method in Section III-A, we solve the above optimization problem based on SDR and SCA. Introducing auxiliary variables ξ , d_j , and $\tau_{i,j}$, we get

$$\max_{\hat{\mathbf{V}}} \xi \quad (33a)$$

$$\text{s.t. } \xi \leq \psi_j - m_{i,j}, \forall j \neq i, j, i \in \mathcal{K} \quad (33b)$$

$$d_j \leq \frac{\text{Tr}(\hat{\mathbf{H}}_{j,j} \hat{\mathbf{V}})}{1 + \sum_{l \neq j} \text{Tr}(\hat{\mathbf{H}}_{j,l} \hat{\mathbf{V}})}, \forall j \in \mathcal{K} \quad (33c)$$

$$\psi_j \leq \log_2(1 + d_j), \forall j \in \mathcal{K} \quad (33d)$$

$$1 + \text{Tr}(\hat{\mathbf{H}}_{i,j} \hat{\mathbf{V}}) \leq \tau_{i,j}, \forall j \neq i, j, i \in \mathcal{K} \quad (33e)$$

$$\log_2(\tau_{i,j}) \leq m_{i,j}, \forall j \neq i, j, i \in \mathcal{K} \quad (33f)$$

$$(31b), (31d) \quad (33g)$$

For the non-convex constraints (33d) and (33f), we obtain a locally optimal solution to the non-convex problem by an iterative optimization method. We solve the following SDP problem in the n th iteration,

$$Q_{\hat{\mathbf{V}}}^{(n)} = \max_{\hat{\mathbf{V}}} \xi \quad (34a)$$

$$\text{s.t. } x'_{j,1} \leq \text{Tr}(\hat{\mathbf{H}}_{j,j} \hat{\mathbf{V}}), \forall j \in \mathcal{K} \quad (34b)$$

$$1 + \sum_{l \neq j} (\tau_{j,l} - 1) \leq x'_{j,2}, \forall j \in \mathcal{K} \quad (34c)$$

$$\frac{1}{2} (\eta_j^{(n)} t_j^2 + \frac{x_{j,2}^2}{\eta_j^{(n)}}) \leq x'_{j,1}, \forall j \in \mathcal{K} \quad (34d)$$

$$\psi_j \leq \log_2(1 + t_j), \forall j \in \mathcal{K} \quad (34e)$$

$$\log_2(\varepsilon'_{i,j}{}^{(n)}) + \frac{\tau_{i,j} - \varepsilon'_{i,j}{}^{(n)}}{\varepsilon'_{i,j}{}^{(n)} \ln 2} \leq m_{i,j}, \forall j \neq i, j, i \in \mathcal{K} \quad (34f)$$

$$(33b), (33e), (31b), (31d), \quad (34g)$$

where $\eta_j^{(n)} = x'_{j,2}{}^{(n-1)} / d_j^{(n-1)}$, $\varepsilon'_{i,j}{}^{(n)} = \tau_{i,j}^{(n-1)}$. Similarly, we can use the CVX toolbox for optimization.

2) *Gaussian Randomization* In Algorithm 2, we drop the rank-one constraint. The rank of the optimal solution $\{\hat{\mathbf{V}}^*\}$ may not be 1. If $\text{Rank}(\hat{\mathbf{V}}^*) = 1$, the corresponding beamforming vector can be obtained by matrix decomposition, i.e., $\hat{\mathbf{V}}^* = \hat{\mathbf{V}}^* \hat{\mathbf{V}}^{*(H)}$. Otherwise, the beamforming vector can be extracted by the Gaussian randomization.

Algorithm 3 The overall optimization algorithm for solving \mathbf{V}_l^H and \mathbf{w}_j

- 1: **Input:** The maximum number of iterations Q , P_j , $\mathbf{h}_{j,i}^H \in \mathbb{C}^{1 \times M}$, $\mathbf{H}_{i,r_l} \in \mathbb{C}^{N \times M}$, $\mathbf{h}_{r_l,j}^H \in \mathbb{C}^{1 \times N}$, σ_0^2 , and $e^{j\tilde{w}}$
- 2: **Output:** The optimal solution $\{\hat{\mathbf{V}}^*\}$
- 3: Initialize the reflection coefficient $\{\Phi_l^{(0)}\}$ of each RIS, and get the Corresponding vector $\tilde{\mathbf{V}}^{(0)}$, $q = 1$
- 4: **repeat**
- 5: For a given $\tilde{\mathbf{V}}^{(q-1)}$, use Algorithm 1 to solve (29) and obtain $\{\mathbf{W}_j^{(q)}\}$
- 6: If $\text{Rank}(\mathbf{W}_j^{(q)}) \neq 1$, use Gaussian randomization decomposition to obtain $\{\mathbf{w}_j^{(q)}\}$.
- 7: For a given $\{\mathbf{w}_j^{(q)}\}$, use Algorithm 2 to solve (34) and obtain $\hat{\mathbf{V}}^{(q)}$.
- 8: If $\text{Rank}(\hat{\mathbf{V}}^{(q)}) \neq 1$, use Gaussian randomization decomposition to obtain $\tilde{\mathbf{V}}^{(q)}$.
- 9: Update $q = q + 1$.
- 10: **until** $q \geq Q$, obtain the optimal $\tilde{\mathbf{V}}^*$, $\{\mathbf{w}_j^{(*)}\}$;
- 11: Solve for $\{\Phi_l^{(*)}\}$ according to $\tilde{\mathbf{V}}^H = e^{j\tilde{w}}[\mathbf{V}^H, 1]$.

C. The Overall Algorithm

In summary, the algorithm for solving (14) based on AO is given in Algorithm 3, where ε is a small threshold and Q is the maximum number of iterations. \mathbf{V}^* is solved according to $\tilde{\mathbf{V}}^H = e^{j\tilde{w}}[\mathbf{V}^H, 1]$ after obtaining the optimal $\tilde{\mathbf{V}}^*$.

1) Convergence Analysis

The optimal target value in the m th iteration is $\xi(\mathbf{w}_j^{(m)}, \mathbf{V}_l^{(m)})$, where $(\mathbf{w}_j^{(m)}, \mathbf{V}_l^{(m)})$ is the feasible solution in the m th iteration. In the $(m+1)$ th iteration, $(\mathbf{w}_j^{(m+1)}, \mathbf{V}_l^{(m+1)})$ is the feasible solution to (29) and $(\mathbf{w}_j^{(m+1)}, \mathbf{V}_l^{(m+1)})$ is the feasible solution to (34).

Then we can get $C(\mathbf{w}_j^{(m)}, \mathbf{V}_l^{(m)}) \stackrel{(a)}{\leq} C(\mathbf{w}_j^{(m+1)}, \mathbf{V}_l^{(m)}) \stackrel{(b)}{\leq} C(\mathbf{w}_j^{(m+1)}, \mathbf{V}_l^{(m+1)})$. The inequality (a) and (b) are established due to the convergence of the SCA in step 3 [29]. Therefore, the target value $\xi^{(m+1)}$ is not less than $\xi^{(m)}$, i.e., $\{\xi^{(m)}\}$ is monotonically non-decreasing. Considering that the total transmit power is limited and the RIS is passive, there is an upper bound on the secrecy performance. So the optimization algorithm 3 is convergent, which can also be verified by the following simulation.

2) Complexity Analysis

The complexity of an SDP problem which has m constraints and each constraint contains an $n \times n$ positive semidefinite matrix is $\mathcal{O}(\sqrt{n} \log \frac{1}{\varepsilon} (mn^3 + m^2n^2 + m^3))$ [30]. Therefore, the computational complexity of this alternating optimization algorithm in each iteration is $\mathcal{O}(\log \frac{1}{\varepsilon} ((\sqrt{M} + \sqrt{N})(K^2 + 3K)^3 + (M^{\frac{5}{2}} + N^{\frac{5}{2}})K^3))$.

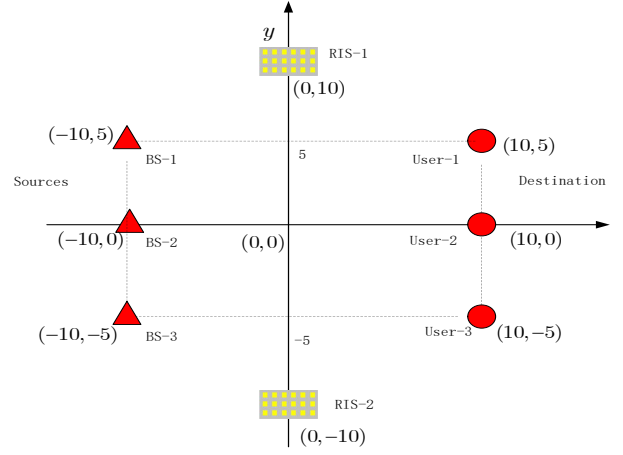


Fig. 2. Simulation setup.

IV. TRANSMISSION STRATEGY UNDER DISCRETE RIS PHASE SHIFTS

It is costly in practice to achieve continuous reflecting coefficients on the reflecting elements due to the hardware limitation. Hence, applying the discrete coefficients on the reflecting elements is more practical. Here, the continuous and discrete phase shift solution sets are denoted as Φ_c and Φ_d , respectively. The system performance with Φ_c serves as the upper bound to that with Φ_d .

The design of discrete phase shifts is a combinatorial optimization problem. We can choose an exhaustive search for the optimization scheme, or use heuristic algorithms such as genetic and simulated annealing algorithms to obtain the optimal solution. However, the search complexity is very high when the numbers of reflecting elements and discrete bits of each element are large. We can apply the projection method to project the solution of (34) with continuous reflecting coefficient Φ_c into discrete reflecting coefficient Φ_d directly. The discrete phase shift is expressed as

$$v_{m,\Phi_d} = \begin{cases} e^{j\theta_m^*}, & m = 1, \dots, M \\ 1, & m = M + 1, \end{cases} \quad (35)$$

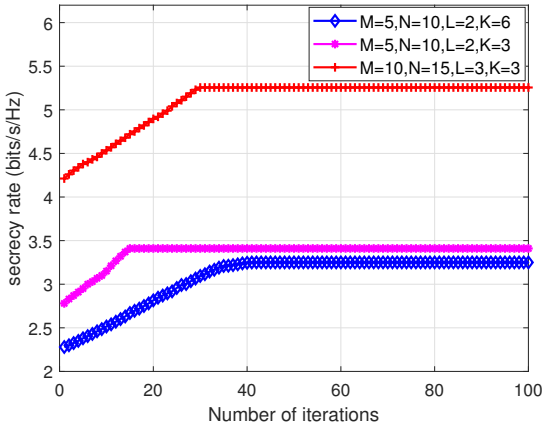
where $\theta_m^* = \arg \min |\theta - \text{angle}(v_{m,\Phi_c})|$. However, the v_{m,Φ_d} obtained by the projection method is not necessarily a optimal local solution. In order to keep the target value non-increasing for Φ_d in each iteration, we update v_{Φ_d} only if $\eta_{\Phi_d}(\{\mathbf{w}_k^{l+1}\}, v_{\Phi_d}^{l+1}) \geq \eta_{\Phi_d}(\{\mathbf{w}_k^{l+1}\}, v_{\Phi_d}^l)$.

V. SIMULATION RESULTS

The location setup for the simulated network is shown in Fig. 2. We consider three paired users and two RISs which are located in the system' South and North at (0, 10) and (0, -10) in meters (m). The channel fading matrix \mathbf{h}_{ij} from the node i to j is modeled as $\mathbf{h}_{ij} = \sqrt{L_0 d_{ij}^{-c_{ij}}} \mathbf{g}_{ij}$, where $L_0 = -30$ dB is the path loss at the reference distance $d_0 = 1$ m. The distance between the node i to j is denoted by d_{ij} while c_{ij} is the corresponding large-scale fading path loss exponent. The

TABLE I
 SYSTEM PARAMETERS.

Carrier center frequency	2.4 GHz
The maximum transmission power	$P_i = P_{\max}$
Maximum number of iterations	$Q = 50$
Path loss exponent c_{ij} with LOS and without LoS	2, 4
Rician factor β_{ij} with LOS and without LoS	3, 0
Noise power σ_j^2 at each user	-90 dBm


 Fig. 3. Convergence of the proposed algorithm for different values of M , N , L , and K with $P_{\max} = 20$ dBm.

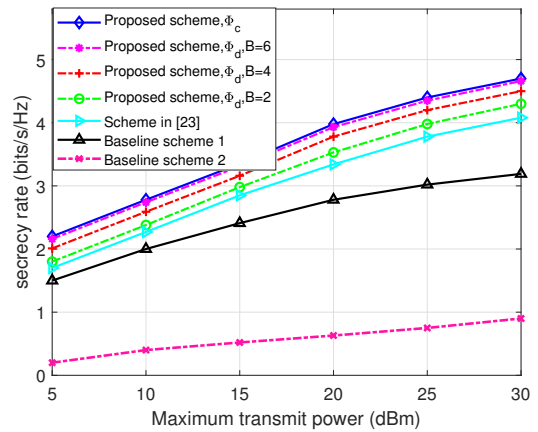
small-scale fading \mathbf{g}_{ij} obeys Rician fading with the Rician factor β_{ij} and is modeled as follows

$$\mathbf{g}_{ij} = \sqrt{\frac{\beta_{ij}}{1 + \beta_{ij}}} \mathbf{g}_{ij}^{\text{LOS}} + \sqrt{\frac{1}{1 + \beta_{ij}}} \mathbf{g}_{ij}^{\text{NLOS}}, \quad (36)$$

where $\mathbf{g}_{ij}^{\text{LOS}}$ and $\mathbf{g}_{ij}^{\text{NLOS}}$ are the line-of-sight (LOS) component of the direct path and Rayleigh non-LOS (NLOS) component, respectively. The LOS and NLOS components are modeled as the product of the array response vectors of the transceivers and Rayleigh fading, respectively. The other channels in the system are generated in a similar manner. Other system parameters used for our simulations are listed in Table 1.

We compare with the other two baseline schemes. For baseline scheme 1, we perform a simple beamforming design without iterative optimization. In particular, we adopt maximum ratio transmission (MRT) for transmit beamforming, i.e., we set $\mathbf{w}_j = \sqrt{P_j} \hat{\mathbf{H}}_{j,j} / \|\hat{\mathbf{H}}_{j,j}\|$ and implement the RISs with random phases. For baseline scheme 2, we consider the system performance when there are no RISs deployed. We optimize the beamforming vector and RIS matrix by setting $\Phi_l = \mathbf{I}_N$ and solve problem (14).

As shown in Fig. 3, we investigate the convergence of the proposed algorithm for different numbers of transmitting antennas M , reflecting elements of each RIS N , and RISs L under the continuous reflecting coefficients. As can be observed from Fig. 3, the proposed algorithm converges monotonically for all M , N , and L . In particular, the algorithm converges after around 15 iterations on average when


 Fig. 4. Secrecy rate versus the maximum transmit power of the BS with $M = 10$, $N = 15$, $L = 2$, $K = 3$.

$M = 5$, $N = 10$, $L = 2$, $K = 3$. For the case with more transmit antennas and RIS reflecting elements, i.e., $M = 10$, $N = 15$, $L = 3$, $K = 3$, the proposed algorithm converges after 30 iterations on average since the dimensions of the solution space of (29) and (34) increase with M and N . The algorithm needs more iterations to converge when $M = 5$, $N = 10$, $L = 2$, $K = 6$ since the numbers of optimization variables and constraints of (29) and (34) increase with the number of user pairs K . In conclusion, the number of iterations required for the proposed algorithm to converge is more affected by the number of paired users than the number of transmit antennas and RIS reflecting elements.

In Fig. 4, we show the secrecy rate versus the maximum transmit power at the AP. It can be seen that the secrecy rate increases monotonically with P_{\max} since the signal-to-interference-plus-noise ratios (SINR) of the target user can be improved by providing it with more transmit power. In addition, the performance gap between continuous and discrete phase shifts increases as B decreases since the RIS phase shift can be adjusted more accurately with more quantization bits. Our proposed scheme outperforms the algorithm in [23] which assumes one RIS with $N = 15$ in the considered range. We also observe that the secrecy rate of our proposed scheme exceeds that of the two baseline schemes. In particular, the fixed MRT beamforming scheme can not make full use of the additional DoF introduced by the extra transmit power. In fact, the MRT beamforming scheme does not mitigate the interference of other users. For baseline scheme 2, the performance loss compared to the proposed scheme is mainly because the target user channel is not greatly enhanced without RIS deployment. Besides, we know the performance gap between the system with RISs and that without RISs increases with the transmit power, which validates the advantages of the introduced RISs. We achieve the balance of the maximum secrecy rate by deploying RISs and optimally designing reflection coefficient matrices.

In Fig. 5, we compare the secrecy rate of deploying a single RIS, two RISs, and three RISs, respectively, under the same total number of RIS elements. We assume that there

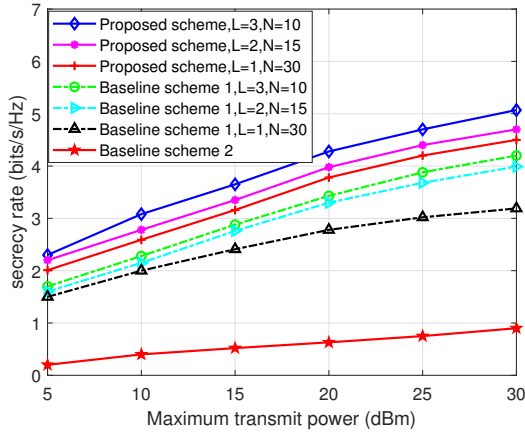


Fig. 5. Secrecy rate versus P_{\max} under the same total number of RIS elements with $M = 10$, $K = 3$.

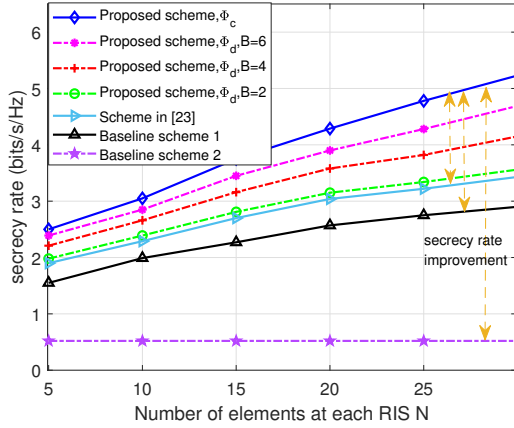


Fig. 6. Secrecy rate versus number of RIS's elements N with $M = 10$, $L = 2$, $K = 3$, $P_{\max} = 20$ dBm.

are $N \times L = 30$ reflecting elements in total. For the scenario when only one RIS with thirty reflecting elements is deployed, it is located in the system's center, i.e., $(0, 0)$. For the scenario when two RISs with fifteen reflecting elements on each RIS are deployed, they are located in the system's South and North, as shown in Fig. 2. The three RISs with ten reflecting elements on each RIS are located in the system's South, North, and center, respectively. As can be observed in Fig. 5, the proposed scheme considerably outperforms both baseline schemes for all three scenarios. In addition, it is beneficial to deploy more RISs under the same number of elements. This is because multiple RISs create multiple independent propagation paths, which introduce macro-diversity and additional spatial DoF. Moreover, the distance between each user and its nearest RIS will be reduced. Although the distance between other interfering users and the nearest RIS is also reduced, our proposed algorithm effectively worsens the eavesdropper's channel quality, which improves the secrecy rate.

Fig. 6 shows the relationship between the secrecy rate and the number of RIS elements N . We can see that the secrecy rate increases with N while remaining unchanged when there's

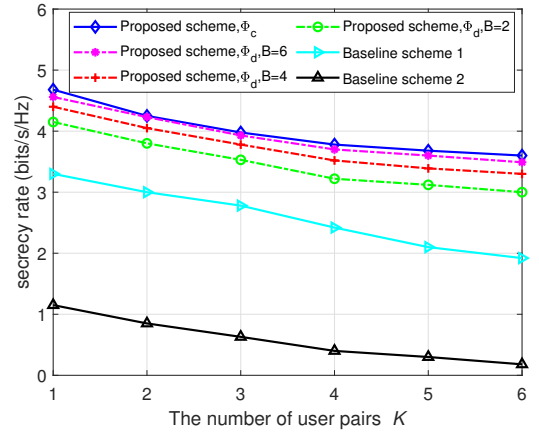


Fig. 7. Secrecy rate versus the number of user pairs K with $M = 10$, $N = 15$, $L = 2$, $P_{\max} = 20$ dBm.

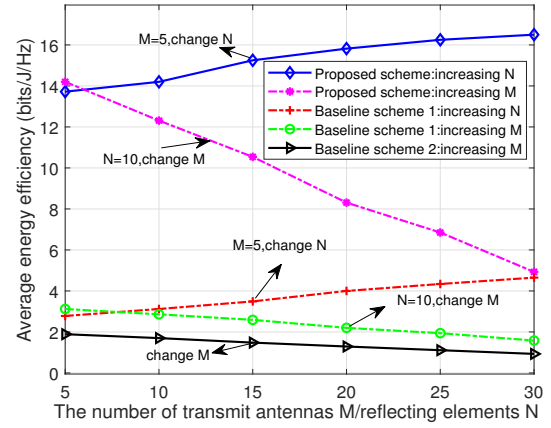


Fig. 8. Average energy efficiency (bits/J/Hz) versus the number of antennas M or reflecting elements N for $K = 3$, $L = 2$.

no RIS because a higher array gain can be achieved with larger N , resulting in greater spatial DoF. The performance gap between continuous phase shift and discrete phase shift schemes increases as the quantization bits B decreases, especially for larger N . When the number of reflecting elements is larger, we need a higher quantization level to achieve a more precise adjustment to obtain a higher array gain. Our scheme outperforms the algorithm in [23] and the baseline schemes.

Fig. 7 plots the secrecy rate versus the number of user pairs K . First, we observe that the secrecy rate achieved by the proposed scheme and both baseline schemes decreases as K increases, due to the fact that the beamforming gain and array gain need to be shared with more users. Moreover, similar to Fig. 6, we can observe that the performance of our proposed scheme with continuous reflecting coefficients is better than that with discrete reflecting coefficients and other baseline schemes. In addition, the reduction rate of the system secrecy rate is substantially lower for the proposed schemes compared to the baseline scheme since RIS can provide higher array gains and more design DoF to deliberately manipulate the wireless communication channels.

In Fig. 8, we investigate the energy efficiency versus the number of antennas M at the BS and the number of reflecting elements N at the RIS. We define the energy efficiency (bits/J/Hz) as the ratio of the maximum secrecy rate to the total power consumption of the system [31]

$$\eta = \frac{\xi(\mathbf{w}_j^{(Q)}, \mathbf{V}_l^{(Q)})}{\frac{1}{\gamma}P + MP_t + P_s + P_c}, \quad (37)$$

where γ is the power amplifier efficiency, P_t is the power consumption of the corresponding RF chain introduced by one antenna element, P_s is the static circuit power of the BS, and P_c is the power consumption of the RIS controller. We set $\gamma = 0.41$, $P_t = 25$ mW, $P_s = 20$ mW, and $P_c = 28$ mW. In Fig.8, we show the average energy efficiency as a function of the number of transmit antennas for $N = 10$ RIS reflecting elements and as a function of the number of reflecting elements at the RIS for $M = 5$ transmit antennas. We can observe that the energy efficiency increases with the number of RIS elements since RISs are passive devices, and more phase shifters can reflect more power received from the BSs, which improves the beamforming gain. In contrast, the energy efficiency is a monotone decreasing function with respect to the number of transmit antennas. This is mainly because more power-consuming RF chains are required as the number of transmit antennas increases, which greatly exceeds the secrecy rate gain. The RIS-assisted wireless network provides lower costs compared with the existing multi-antenna wireless systems and leads to less overhead.

VI. CONCLUSION

In this paper, we deploy multiple RISs to improve the secrecy rate in a multi-user MISO system with multiple paired transceivers with confidential information. We jointly optimize the transmit beamforming and RIS reflecting coefficient matrix to maximize the minimum secrecy rate of all the users in the system. We employ an alternating optimization approach to address the non-convexity due to the coupled optimization variables. In particular, we optimally design the transmit beamforming and RIS phase shift based on SDR and SCA. We prove and verify the convergence of the proposed iterative optimization algorithm. The simulation results show the advantages of RIS in improving PLS. Furthermore, the deployment of multiple RISs under the same number of RIS elements was shown to be favorable for enhancing physical layer security, which exploits macro-diversity gains and extra spatial degrees of freedom.

REFERENCES

- [1] X. Chen, D. W. K. Ng, W. H. Gerstacker, and H. -H. Chen, "A survey on multiple-antenna techniques for physical layer security," *IEEE Commun. Surveys Tuts.*, vol. 19, no. 2, pp. 1027–1053, 2017.
- [2] A. D. Wyner, "The wire-tap channel," *The Bell Syst. Technical J.*, vol. 54, no. 8, pp. 1355–1387, Oct. 1975.
- [3] H. Du *et al.*, "On the distribution of the ratio of products of Fisher-Snedecor F random variables and its applications," *IEEE Trans. Veh. Technol.*, vol. 69, no. 2, pp. 1855–1866, Feb. 2020.
- [4] J. Li, A. P. Petropulu, and S. Weber, "On cooperative relaying schemes for wireless physical layer security," *IEEE Trans. Signal Process.*, vol. 59, no. 10, pp. 4985–4997, Oct. 2011.
- [5] Z. Zhu, Z. Chu, N. Wang, S. Huang, Z. Wang, and I. Lee, "Beamforming and power splitting designs for AN-aided secure multi-user MIMO SWIPT systems," *IEEE Trans. Inf. Forensics Security*, vol. 12, no. 12, pp. 2861–2874, Dec. 2017.
- [6] L. Dong, Z. Han, A. P. Petropulu, and H. V. Poor, "Improving wireless physical layer security via cooperating relays," *IEEE Trans. Signal Process.*, vol. 58, no. 3, pp. 1875–1888, Mar. 2010.
- [7] T. J. Cui, M. Q. Qi, X. Wan, J. Zhao, and Q. Cheng, "Coding metamaterials, digital metamaterials and programmable metamaterials," *Light: Sci. Applicat.*, vol. 3, no. 10, p. e218, 2014.
- [8] M. Najafi, V. Jamali, R. Schober, and H. V. Poor, "Physics-based modeling and scalable optimization of large intelligent reflecting surfaces," *IEEE Trans. Commun.*, vol. 69, no. 4, pp. 2673–2691, Apr. 2021.
- [9] S. Asaad, R. F. Schaefer, and H. Vincent Poor, "Hybrid precoding for secure transmission in reflect-array-assisted massive MIMO systems," in *Proc. IEEE ICASSP*, 2020, pp. 8693–8697.
- [10] J. Zhang *et al.*, "Prospective multiple antenna technologies for beyond 5G," *IEEE J. Sel. Areas Commun.*, vol. 38, no. 8, pp. 1637–1660, Aug. 2020.
- [11] Q. Wu and R. Zhang, "Intelligent reflecting surface enhanced wireless network via joint active and passive beamforming," *IEEE Trans. Wireless Commun.*, vol. 18, no. 11, pp. 5394–5409, Nov. 2019.
- [12] C. Huang, A. Zappone, G. C. Alexandropoulos, M. Debbah, and C. Yuen, "Reconfigurable intelligent surfaces for energy efficiency in wireless communication," *IEEE Trans. Wireless Commun.*, vol. 18, no. 8, pp. 4157–4170, Aug. 2019.
- [13] S. Abeywickrama, R. Zhang, Q. Wu, and C. Yuen, "Intelligent reflecting surface: Practical phase shift model and beamforming optimization," *IEEE Trans. Commun.*, vol. 68, no. 9, pp. 5849–5863, Sep. 2020.
- [14] X. Yu, D. Xu, and R. Schober, "Enabling secure wireless communications via intelligent reflecting surfaces," in *Proc. IEEE GLOBECOM*, pp. 1–6, 2019.
- [15] M. Cui, G. Zhang, and R. Zhang, "Secure wireless communication via intelligent reflecting surface," *IEEE Wireless Commun. Lett.*, vol. 8, no. 5, pp. 1410–1414, Oct. 2019.
- [16] H. Niu, Z. Chu, F. Zhou, and Z. Zhu, "Simultaneous transmission and reflection Reconfigurable intelligent surface assisted secrecy MISO networks," *IEEE Commun. Lett.*, vol. 25, no. 11, pp. 3498–3502, Nov. 2021.
- [17] H. Niu, Z. Chu, F. Zhou, Z. Zhu, M. Zhang, and K. -K. Wong, "Weighted sum secrecy rate maximization Using intelligent reflecting surface," *IEEE Trans. Commun.*, vol. 69, no. 9, pp. 6170–6184, Sep. 2021.
- [18] X. Yu, D. Xu, Y. Sun, D. W. K. Ng, and R. Schober, "Robust and secure wireless communications via Intelligent Reflecting Surfaces," *IEEE J. Sel. Areas Commun.*, vol. 38, no. 11, pp. 2637–2652, Nov. 2020.
- [19] J. Zhang, H. Du, Q. Sun, B. Ai, and D. W. K. Ng, "Physical layer security enhancement with reconfigurable intelligent surface-aided networks," *IEEE Trans. Inf. Forensics Security*, vol. 16, pp. 3480–3495, 2021.
- [20] A. Mukherjee, S. A. A. Fakoorian, J. Huang, and A. L. Swindlehurst, "Principles of physical layer security in multiuser wireless networks: A Survey," *IEEE Commun. Surveys Tuts.*, vol. 16, no. 3, pp. 1550–1573, 2014.
- [21] W. Huang, Y. Zeng, and Y. Huang, "Achievable rate region of MISO interference channel aided by intelligent reflecting surface," *IEEE Trans. Veh. Technol.*, vol. 69, no. 12, pp. 16264–16269, Dec. 2020.
- [22] J. Zhang *et al.*, "Deep reinforcement learning-empowered beamforming design for IRS-assisted MISO interference channels," in *Proc. WCSP*, 2021, pp. 1–5.
- [23] Y. Jia, C. Ye, and Y. Cui, "Analysis and optimization of an intelligent reflecting surface-assisted system with interference," *IEEE Trans. Wireless Commun.*, vol. 19, no. 12, pp. 8068–8082, 2020.
- [24] M. A. ElMossallamy *et al.*, "RIS optimization on the complex circle manifold for interference mitigation in interference channels," *IEEE Trans. Veh. Technol.*, vol. 70, no. 6, pp. 6184–6189, Jun. 2021.
- [25] H. Zhang *et al.*, "Channel estimation with simultaneous reflecting and sensing reconfigurable intelligent metasurfaces," in *Proc. IEEE SPAWC*, 2021, pp. 536–540.
- [26] Z. He and X. Yuan, "Cascaded channel estimation for large intelligent metasurface assisted massive MIMO," *IEEE Wireless Commun. Lett.*, vol. 9, no. 2, pp. 210–214, Feb. 2020.
- [27] S. Vishwanath, N. Jindal, and A. Goldsmith, "Duality, achievable rates, and sum-rate capacity of Gaussian MIMO broadcast channels," *IEEE Trans. Inf. Theory*, vol. 49, no. 10, pp. 2658–2668, Oct. 2003.
- [28] Z. Luo *et al.*, "Semidefinite relaxation of quadratic optimization problems," *IEEE Signal Process. Mag.*, vol. 27, no. 3, pp. 20–34, 2010.

- [29] B. Li, Z. Fei, Z. Chu, and Y. Zhang, "Secure transmission for heterogeneous cellular networks with wireless information and power transfer," *IEEE Systems J.*, vol. 12, no. 4, pp. 3755–3766, Dec. 2018.
- [30] I Pólik and T. Terlaky . "Interior point methods for nonlinear optimization." Lecture Notes in Mathematics -Springer-verlag, 2010.
- [31] D. Nguyen, L. Tran, P. Pirinen, and M. Latva-aho, "Precoding for full duplex multiuser MIMO systems: Spectral and energy efficiency maximization," *IEEE Trans. Signal Process.*, vol. 61, no. 16, pp. 4038–4050, Aug. 2013.



Yi Wang received B.S. degree from Information Engineering University, Zhengzhou, China, in 2006, and the M.S. and Ph.D. degrees from the school of Information Science and Engineering, Southeast University, China, in 2009 and 2016, respectively. Since October 2016 he has been with the faculty of the School of Intelligent Engineering, Zhengzhou University of Aeronautics, China. His current research interests include massive MIMO, energy-efficient communication, UAV-aided communication, physical layer security, wireless power transfer and intelligent reflecting surface-aided wireless communication. He received the best paper awards of the IEEE WCSP in 2015.



Ya Liu received the M.S. degree in Information and Communication Engineering from Harbin Institute of Technology, China, in 2013. She is currently a Lecturer of the School of Intelligent Engineering, Zhengzhou University of Aeronautics, China. She is currently pursuing her Ph.D. degree at the PLA Strategic Support Force Information Engineering University, Zhengzhou, China. Her research interests include physical layer security, secret key generation and reconfigurable intelligent surfaces-aided wireless communication.



Jie Yang received the M.S. degree in Communication Engineering from the College of Communications Engineering, PLA University of Science and Technology, Nanjing, China, in 2017. He is currently pursuing the Ph.D. degree with the National Digital Switching System Engineering and Technological Research and Developing Center, Zhengzhou, China. His major research interests include wireless communication security and secret key generation.



Kaizhi Huang received the B.E. degree in Digital Communication and the M.S. degree in Communication and Information System from the National Digital Switching System Engineering and Technological Research Center (NDSC), in 1995 and 1998, respectively, and the Ph.D. degree in Communication and Information System from Tsinghua University, Beijing, China, in 2003. She has been a Faculty Member of NDSC, since 1998, where she is currently a Professor and the Director of the Laboratory of Mobile Communication Networks. Her research interests include wireless network security and signal processing.



Xiaoli Sun was born in 1992. She received the Ph.D. degree from Army Engineering University of PLA. She is currently a Lecturer of PLA Strategic Support Force Information Engineering University, Zhengzhou, China. Her research interests include wireless communications and physical layer security.